

The Journal of Neuroscience

<https://jneurosci.msubmit.net>

Statistics of natural communication signals observed in the wild identify important yet neglected stimulus regimes in weakly electric fish

Jan Benda, Eberhard Karls Universität Tübingen  
Jörg Henninger, Eberhard Karls Universität Tübingen  
Rüdiger Krahe, Humboldt-Universität zu Berlin  
Frank Kirschbaum, Humboldt-Universität zu Berlin  
Jan Grewe, Eberhard-Karls-Universität Tübingen

Commercial Interest:

1 Statistics of natural communication signals observed in the wild identify  
2 important yet neglected stimulus regimes in weakly electric fish

3 Jörg Henninger<sup>1</sup>, Rüdiger Krahe<sup>2,3</sup>, Frank Kirschbaum<sup>2</sup>, Jan Grewe<sup>1</sup>, Jan Benda<sup>1†</sup>

4 <sup>1</sup> Institut für Neurobiologie, Eberhard Karls Universität, Auf der Morgenstelle 28E, 72076 Tübingen, Germany

5 <sup>2</sup> Institut für Biologie, Humboldt-Universität zu Berlin, Philippstr. 13, 10115 Berlin, Germany

6 <sup>3</sup> McGill University, Department of Biology, 1205 Ave. Docteur Penfield, Montreal, Quebec H3A 1B1, Canada

7 † corresponding authors: [jan.benda@uni-tuebingen.de](mailto:jan.benda@uni-tuebingen.de), [joerg.henninger@posteo.de](mailto:joerg.henninger@posteo.de)

8	Number of pages	25	Number of words abstract	168
	Number of figures	8	Number of words introduction	451
	Number of tables	0	Number of words discussion	1499
	Number of multimedia	5		
	Number of extended data figures	3		

9 ***Competing interests***

10 The authors declare no competing financial interests.

11 ***Acknowledgment***

12 Supported by the BMBF Bernstein Award Computational Neuroscience 01GQ0802 to J.B., a Discovery Grant  
13 from the Natural Sciences and Engineering Research Council of Canada to RK, and a Short Time Fellowship to  
14 J.H. from the Smithsonian Tropical Research Institute. We thank Hans Reiner Polder and Jürgen Planck from npi  
15 electronic GmbH for designing the amplifier, Sophie Picq, Diana Sharpe, Luis de León Reyna, Rigoberto González,  
16 Eldredge Bermingham, the staff from the Smithsonian Tropical Research Institute, and the Emberá community of  
17 Peña Bijagual for their logistical support, Fabian Sinz for advice on the analysis, and Ulrich Schnitzler and Janez  
18 Presern for comments on the manuscript.

## Abstract

Sensory systems evolve in the ecological niches each species is occupying. Accordingly, encoding of natural stimuli by sensory neurons is expected to be adapted to the statistics of these stimuli. For a direct quantification of sensory scenes we tracked natural communication behavior of the weakly electric fish, *Apteronotus rostratus*, in their Neotropical rainforest habitat with high spatio-temporal resolution over several days. In the context of courtship we observed large quantities of electrocommunication signals. Echo responses, acknowledgment signals, and their synchronizing role in spawning demonstrated the behavioral relevance of these signals. In both courtship and aggressive contexts, we observed robust behavioral responses in stimulus regimes that have so far been neglected in electrophysiological studies of this well characterized sensory system and that are well beyond the range of known best frequency and amplitude tuning of the electroreceptor afferents' firing rate. Our results emphasize the importance of quantifying sensory scenes derived from freely behaving animals in their natural habitats for understanding the function and evolution of neural systems.

**Keywords** sensory systems | animal communication | sexual dimorphism | *Apteronotus* | chirp

## Significance statement

The processing mechanisms of sensory systems have evolved in the context of the natural lives of organisms. To understand the functioning of sensory systems therefore requires probing them in the stimulus regimes they evolved in. We took advantage of the continuously generated electric fields of weakly electric fish to explore electrosensory stimulus statistics in their natural Neotropical habitat. Unexpectedly, many of the electrocommunication signals recorded during courtship, spawning, and aggression had much smaller amplitudes or higher frequencies than stimuli used so far in neurophysiological characterizations of the electrosensory system. Our results demonstrate that quantifying sensory scenes derived from freely behaving animals in their natural habitats is essential to avoid biases in the choice of stimuli used to probe brain function.

## Introduction

Sensory systems evolve in the context of species-specific natural sensory scenes (Lewicki et al., 2014). Consequently, naturalistic stimuli have been crucial for advances in understanding the design and function of neural circuits in sensory systems, in particular the visual (Laughlin, 1981; Olshausen and Field, 1996; Gollisch and Meister, 2010; Froudarakis et al., 2014) and the auditory system (Theunissen et al., 2000; Smith and Lewicki, 2006; Clemens and Ronacher, 2013). Communication signals are natural stimuli that are, by definition, behaviorally relevant (Wilson, 1975; Endler, 1993). Not surprisingly, certain acoustic communication signals, for example, have

48 been reported to evoke responses in peripheral auditory neurons that are highly informative about these stimuli  
49 (Rieke et al., 1995; Machens et al., 2005). However, other stimuli that do not strongly drive sensory neurons may  
50 also be behaviorally relevant and equally important for understanding the functioning of neural systems. Unfortu-  
51 nately, they are often neglected in electrophysiological studies, because they do not evoke obvious neural responses  
52 (Olshausen and Field, 2005).

53 To address this bias, we quantified behaviorally relevant sensory scenes that we recorded in freely interacting  
54 animals in their natural habitat. Tracking the sensory input of freely behaving and unrestrained animals in natural  
55 environments is notoriously challenging (Egnor and Branson, 2016). We took advantage of the continuously gen-  
56 erated electric organ discharge (EOD; Fig. 1 A) of gymnotiform weakly electric fish to track their movements and  
57 electrocommunication signals without the need of tagging individual fish.

58 The quasi-sinusoidal EOD together with an array of electroreceptors distributed over the fish's skin (Carr et al.,  
59 1982) forms an active electrosensory system used for prey capture (Nelson and MacIver, 1999), navigation (Fo-  
60 towat et al., 2013), and communication (Smith, 2013). Both, the EOD alone and its modulations, function as  
61 communication signals that convey information about species, sex, status and intent of individuals (e.g., Hagedorn  
62 and Heiligenberg, 1985; Stamper et al., 2010; Fugère et al., 2011). In *Apteronotus* several types of brief EOD  
63 frequency excursions called “chirps”(Fig. 1 B) have been studied extensively in the laboratory (e.g., Engler and Zu-  
64 panc, 2001) and have been associated with courtship (Hagedorn and Heiligenberg, 1985), aggression (Zakon et al.,  
65 2002), and the deterrence of attacks (Hupé and Lewis, 2008). P-unit tuberous electroreceptors encode amplitude  
66 modulations of the EOD (Bastian, 1981a) as they are induced by the presence of a second fish and by chirps (e.g.  
67 Benda et al., 2005; Walz et al., 2014).

68 Here we describe electrocommunication behavior of weakly electric fish recorded in their natural neotropi-  
69 cal habitat with unprecedented high temporal and spatial resolution. We found extensive chirping interactions on  
70 timescales ranging from tens of milliseconds to minutes in the context of courtship. In a complementary breeding  
71 experiment we confirmed the synchronizing role of chirping in spawning. From the observed courtship and ag-  
72 gression scenes we computed the statistics of interaction distances determining the effective signal amplitudes, and  
73 the signal frequencies driving the electrosensory system. In the discussion we then compare these natural stimulus  
74 statistics with the known coding properties of electroreceptor afferents.

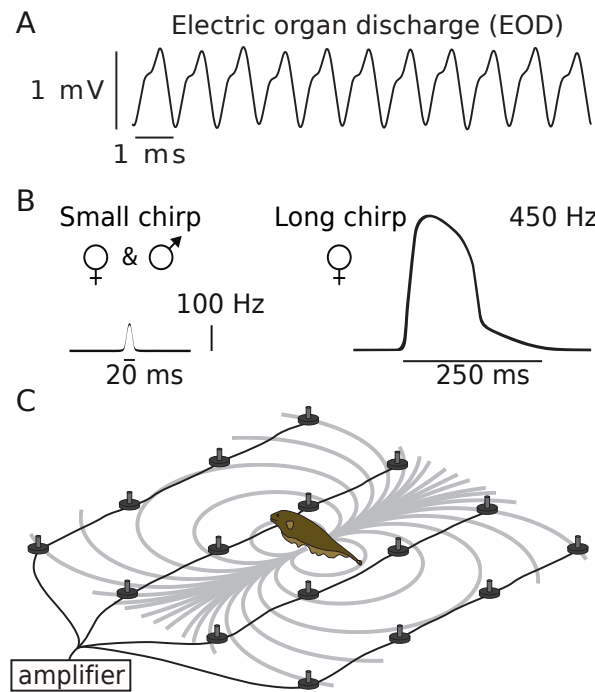


Figure 1: Monitoring electrocommunication behavior in the natural habitat. A) EOD waveform of *A. rostratus*. B) Transient increases of EOD frequency, called small and long chirps, function as communication signals. C) The EOD generates a dipolar electric field (gray isopotential lines) that we recorded with an electrode array, allowing to track individual fish and to monitor communication interactions with high temporal and spatial acuity.

Extended data:

Figure 1 – 1: Field site and the electrode array positioned in a stream.

## 75 **Materials and methods**

### 76 **Field site**

77 The field site is located in the Tuira River basin, Province of Darién, Republic of Panamá (fig. 1 – 1 A), at Que-  
 78 brada La Hoya, a narrow and slow-flowing creek supplying the Chucunaque River. Data were recorded about 2 km  
 79 from the Emberá community of Peña Bijagual and about 5 km upstream of the stream’s mouth ( $8^{\circ}15'13.50''\text{N}$ ,  
 80  $77^{\circ}42'49.40''\text{W}$ ). At our recording site (fig. 1 – 1 B), the water level ranged from 20 – 70 cm. The water tempera-  
 81 ture varied between 25 and 27 °C on a daily basis and water conductivity was stable at 150 – 160  $\mu\text{S}/\text{cm}$ . At this  
 82 field site we recorded four species of weakly electric fish, the pulse-type fish *Brachyhypopomus occidentalis* (about  
 83 30 – 100 Hz pulses per second), the wave-type species *Sternopygus dariensis* (EOD  $f$  at about 40 – 220 Hz), *Eigen-*  
 84 *mannia humboldtii* (200 – 580 Hz), and *Apteronotus rostratus* (580 – 1100 Hz). We here focused exclusively on *A.*

85 *rostratus*, a member of the *A. leptorhynchus* species group (brown ghost knifefish, [de Santana and Vari, 2013](#)).

## 86 **Field monitoring system**

87 Our recording system (Fig. 1 C, fig. 1 – 1 B) consisted of a custom-built 64-channel electrode and amplifier system  
88 (npi electronics GmbH, Tamm, Germany) running on 12 V car batteries. Electrodes were low-noise headstages  
89 encased in epoxy resin (1× gain, 10 × 5 × 5 mm). Signals detected by the headstages were fed into the main  
90 amplifier (100× gain, 1st order high-pass filter 100 Hz, low-pass 10 kHz) and digitized with 20 kHz per channel  
91 with 16-bit amplitude resolution using a custom-built low-power-consumption computer with two digital-analog  
92 converter cards (PCI-6259, National Instruments, Austin, Texas, USA). Recordings were controlled with custom  
93 software written in C++ (<https://github.com/bendalab/fishgrid>) that also saved data to hard disk for offline  
94 analysis (exceeding 400 GB of uncompressed data per day). We used a minimum of 54 electrodes, arranged in an  
95 9 × 6 array covering an area of 240 × 150 cm (30 cm spacing). The electrodes were mounted on a rigid frame  
96 (thermoplast 4 × 4 cm profiles, 60 % polyamid, 40% fiberglass; Technoform Kunststoffprofile GmbH, Lohfelden,  
97 Germany), which was submerged into the stream and fixed in height 30 cm below the water level.

## 98 **Data analysis**

99 All data analysis was performed in Python 2.7 ([www.python.org](http://www.python.org), <https://www.scipy.org/>). Scripts and raw  
100 data (Panamá field data: 2.0 TB, Berlin breeding experiment: 3.7 TB of EOD recordings and 11.4 TB video files)  
101 are available on request, data of the extracted EOD frequencies, position estimates and chirps are available at  
102 <https://web.gin.g-node.org/bendalab>, and some of the core algorithms are accessible at Github under the  
103 GNU general public license (<https://github.com/bendalab/thunderfish>).

104 Summary data are expressed as means ± standard deviation, unless indicated otherwise.

105 Spectrograms in Fig. 3 and Fig. 7 B were calculated from data sampled at 20 kHz in windows of 1024 and 2048  
106 data points, respectively, and shifted by 50 data points.

107 **Fish identification and tracking** First, information about electric fish presence, EOD frequency (EOD*f*), and  
108 approximate position were extracted. Each electrode signal was analyzed separately in sequential overlapping  
109 windows (1.22 s width, 85 % overlap). For each window the power spectral density was calculated (8192 FFT data  
110 points, 5 sub-windows, 50% overlap) and spectral peaks above a given threshold were detected. Individual fish  
111 were extracted from the list of peak frequencies, based on the harmonic structure of wave-type EODs. Finally, fish  
112 detections in successive time windows were matched, combined, and stored for further analysis.

113 **Position estimation** For each fish, the signals of all electrodes were bandpass-filtered (forward-backward but-  
 114 terworth filter, 3rd order,  $5\times$  multipass,  $\pm 7$  Hz width) at the fish's EOD  $f$ . Then the envelope was computed from  
 115 the resulting filtered signal using a root-mean-square filter (10 EOD cycles width). Each 40 ms the fish position  $\vec{x}$   
 116 was estimated from the four electrodes  $i$  with the largest envelope amplitudes  $A_i$  at position  $\vec{e}_i$  as a weighted spatial  
 117 average

$$\vec{x} = \frac{\sum_{i=1}^{n=4} \sqrt{A_i} \cdot \vec{e}_i}{\sum_{i=1}^{n=4} \sqrt{A_i}}$$

118 (movie [M 1](#)). This estimate proved to be the most robust against fish moving close to the edges of the electrode  
 119 array, as verified with both experiments and simulations ([Henninger, 2015](#)). Finally, the position estimates were  
 120 filtered with a running average filter of 200 ms width to yield a smoother trace of movements.

121 **Chirp detection and analysis** For each fish the electrode voltage traces were bandpass-filtered (forward-backward  
 122 butterworth filter, 3rd order,  $5\times$  multipass,  $\pm 7$  Hz width) at the fish's EOD  $f$  and at 10 Hz above the EOD  $f$ . For  
 123 each passband the signal envelope was estimated using a root-mean-square filter over 10 EOD cycles. Rapid  
 124 positive EOD frequency excursions cause the signal envelope at the fish's baseline frequency to drop and in the  
 125 passband above the fish's EOD  $f$  to increase in synchrony with the frequency excursion. If events were detected  
 126 synchronously in both passbands on more than two electrodes, and exceeded a preset amplitude threshold, they  
 127 were accepted as communication signals.

128 Communication signals with a single peak in the upper passband were detected as small chirps. Signals of up  
 129 to 600 ms duration and two peaks in the upper passband, marking the beginning and the end of the longer frequency  
 130 modulation, were detected as long chirps. All chirps in this study were verified manually. However, it is likely that  
 131 some chirps were missed, since detection thresholds were set such that the number of false positives was very low.  
 132 Also, abrupt frequency rises (AFRs, [Engler and Zupanc, 2001](#)) were probably not detected because of their low  
 133 frequency increase.

134 Interchirp-interval probability densities were generated for pairs of fish and only for the time period in which  
 135 both fish were producing chirps. Kernel density histograms of interchirp intervals (Fig. [5 – 1](#)) were computed with  
 136 a Gaussian kernel with a standard deviation of 20 ms.

137 Rates of small chirps before and after female long chirps (Fig. [5 A, C](#)) were calculated by convolving the chirp  
 138 times with a Gaussian kernel ( $\sigma = 0.5$  s) separately for each episode and subsequently calculating the means and  
 139 standard deviations.

140 For quantifying the echo response (Fig. 6) we computed the cross-correlogram

$$r(\tau) = \frac{1}{n_a} \sum_{j=1}^{n_a} \sum_{i=1}^{n_b} g(\tau - (t_{b,i} - t_{a,j}))$$

141 with the  $n_a$  chirp times  $t_{a,j}$  of fish  $a$  and the  $n_b$  chirp times  $t_{b,i}$  of fish  $b$  using a Gaussian kernel  $g(t)$  with a  
 142 standard deviation of 20 ms. To estimate its confidence intervals, we repeatedly resampled the original dataset  
 143 (2000 times jackknife bootstrapping; random sampling with replacement), calculated the cross-correlogram as  
 144 described above and determined the 2.5 and 97.5 % percentiles. To create the cross-correlograms of independent  
 145 chirps, we repeatedly (2000 times) calculated the cross-correlograms on chirps jittered in time by adding a random  
 146 number drawn from a Gaussian distribution with a standard deviation of 500 ms and determined the mean and  
 147 the 2.5 and 97.5 % percentiles. Deviations of the observed cross-correlogram beyond the confidence interval of  
 148 the cross-correlogram of jittered chirp times are significant on a 5 % level, and are indicative of an echo response.  
 149 Reasonable numbers of chirps for computing meaningful cross-correlograms (more than several hundreds of chirps)  
 150 were available in five pairs of fish.

151 **Beat frequencies and spatial distances** The distance between two fish at the time of each chirp (Fig. 8 B) was  
 152 determined from the estimated fish positions. The distance estimates were compiled into kernel density histograms  
 153 that were normalized to their maximal value. The Gaussian kernel had a standard deviation of 1 cm for courtship  
 154 small chirps, and 2 cm for courtship long chirps as well as intruder small chirps. Distances between the intruding  
 155 male and the courting male during assessment behavior (Fig. 8 C, top) were measured every 40 ms beginning with  
 156 the appearance of the intruding fish until the eventual approach or attack. These distances, collected from a total  
 157 assessment time of 923 s, were summarized in a kernel density histogram with Gaussian kernels with a standard  
 158 deviation of 2 cm.

159 Attack distances between two males (Fig. 8 C, bottom) were determined at the moment a resident male initiated  
 160 its movement toward an intruding male. This moment was clearly identifiable as the onset of a linear movement of  
 161 the resident male towards the intruder from plots showing the position of the fish as a function of time.

162 The distribution of beat frequencies generated by fish present in the electrode array at the same time (Fig. 8 E)  
 163 was calculated from all recordings. The average frequency difference of each pair of fish simultaneously detected  
 164 in the recordings was compiled into a kernel density histogram with a Gaussian kernel with a standard deviation of  
 165 10 Hz. Similarly, for courtship and aggressive behavior (Fig. 8 F, G) the mean frequency differences were extracted  
 166 for the duration of these interactions.

167 **Electric fields** For an estimation of EOD amplitude as a function of distance, histograms of envelope amplitudes  
168 from all electrodes of the array were computed as a function of distance between the electrodes and the estimated  
169 fish position. For each distance bin in the range of 20 – 100 cm the upper 95 % percentile of the histogram was  
170 determined and a power law was fitted to these data points. Gymnotiform electroreceptors measure the electric  
171 field, i.e., the first spatial derivative of the EOD amplitudes as shown in Fig. 8 A.

### 172 **Breeding monitoring setup**

173 In the laboratory breeding study, we used the brown ghost knifefish *Apteronotus leptorhynchus*, a close relative of  
174 *A. rostratus* (de Santana and Vari, 2013). The two species share many similarities. (i) Most chirps produced by  
175 both species are “small chirps” that in *A. leptorhynchus* have been classified as type-2 chirps (Engler and Zupanc,  
176 2001). (ii) Females of both species additionally generate small proportions of “long chirps”, similar to the type-4  
177 chirps classified for *A. leptorhynchus* males. (iii) Both species show the same sexual dimorphism in EOD*f*.

178 The laboratory setup for breeding *A. leptorhynchus* consisted of a tank (100 × 45 × 60 cm) placed in a darkened  
179 room and equipped with bubble filters and PVC tubes provided for shelter. Water temperature was kept between  
180 21 and 30 °C. The light/dark cycle was set to 12/12 hours. Several pieces of rock were placed in the center of the  
181 tank as spawning substrate. EOD signals were recorded differentially using four pairs of graphite electrodes. Two  
182 electrode pairs were placed on each side of the spawning substrate. The signals were amplified and analog filtered  
183 using a custom-built amplifier (100× gain, 100 Hz high-pass, 10 kHz low-pass; npi electronics GmbH, Tamm,  
184 Germany), digitized at 20 kHz with 16 bit (PCI-6229, National Instruments, Austin, Texas, USA), and saved to  
185 hard disk for offline analysis. The tank was illuminated at night with a dozen infrared LED spotlights (850 nm,  
186 6W, ABUS TV6700) and monitored continuously (movie M4) with two infrared-sensitive high-resolution video  
187 cameras (Logitech HD webcam C310, IR filter removed manually). The cameras were controlled with custom  
188 written software (<https://github.com/bendalab/videoRecorder>) and a timestamp for each frame was saved  
189 for later synchronization of the cameras and EOD recordings. Six fish of *A. leptorhynchus* (three male, three  
190 female; imported from the Río Meta region, Colombia) were kept in a tank for over a year before being transferred  
191 to the recording tank. First, fish were monitored for about a month without external interference. We then induced  
192 breeding conditions (Kirschbaum and Schugardt, 2002) by slowly lowering water conductivity from 830 μS/cm to  
193 about 100 μS/cm over the course of three months by diluting continuously the tank water with deionized water.  
194 The tank was monitored regularly for the occurrence of spawned eggs.

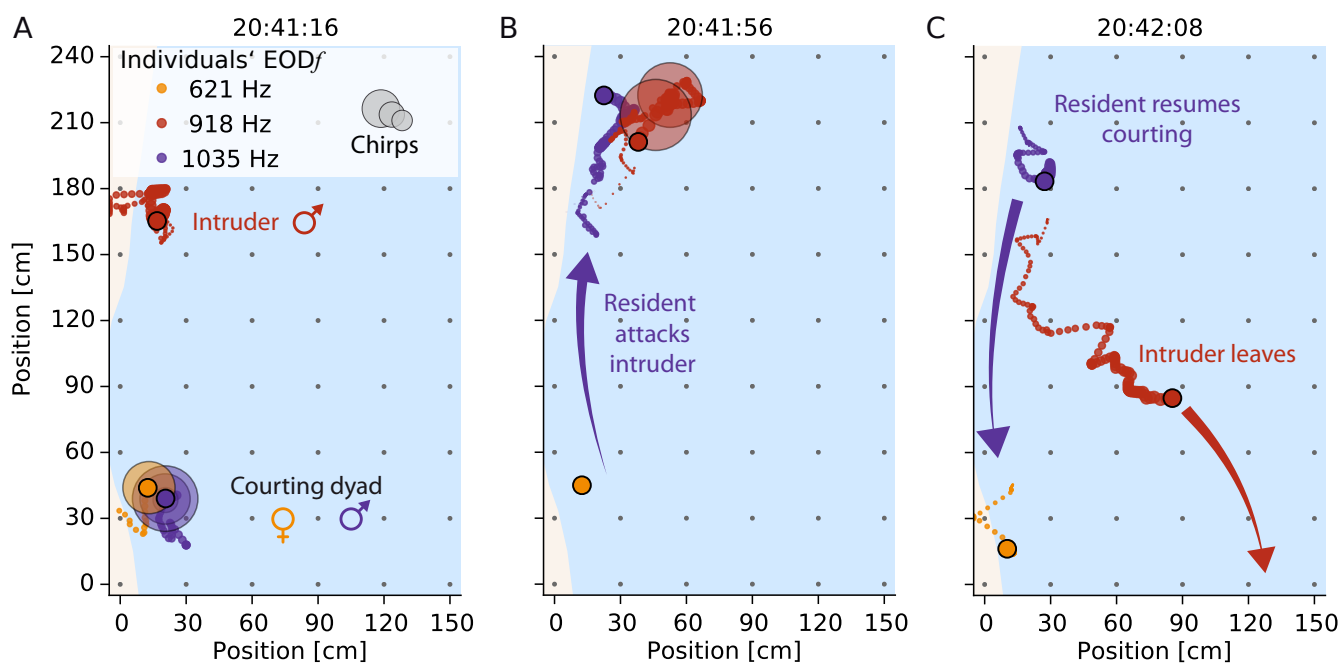


Figure 2: Snapshots of reconstructed interactions of weakly electric fish. See movie [M2](#) for an animation. The current fish position is marked by filled circles. Trailing dots indicate the positions over the preceding 5 s. Colors label individual fish throughout the manuscript. Large transparent circles denote occurrence of chirps. Gray dots indicate electrode positions, and light blue illustrates the water surface. The direction of water flow is from top to bottom. A) Courting female (orange) and male (purple) are engaged in intense chirping activity. An intruder male (red) lingers at a distance of about one meter. B) The courting male attacks (purple arrow) the intruder who emits a series of chirps and, C) leaves the recording area (red arrow), while the resident male resumes courting (purple arrow).

## Results

195

196 We recorded the EODs of weakly electric fish in a stream in the Panamanian rainforest by means of a submerged  
 197 electrode array at the onset of their reproductive season in May, 2012 (Fig. 1 C, Fig. 1 – 1, movie [M1](#)). Individual  
 198 gymnotiform knifefish, *Apteronotus rostratus*, were identified and their movements tracked continuously based on  
 199 the species- and individual-specific frequency of their EOD ( $EODf \approx 580$  to 1050 Hz). In these recordings we  
 200 detected several types of “chirps” emitted during courtship and aggression (Fig. 1 B). This approach allowed us to  
 201 reconstruct social interactions in detail (Fig. 2, movies [M2](#) and [M3](#)) and evaluate the associated sensory scenes  
 202 experienced by these fish in their natural habitat.

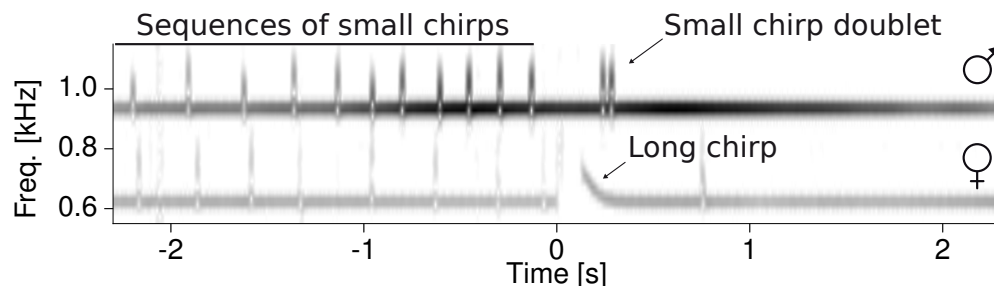


Figure 3: Spectrogram of stereotyped courtship chirping. The example spectrogram (audio [A 1](#)) shows EOD $f$ s of a female (620 Hz, same as in Fig. 2) and a male (930 Hz) and their stereotyped chirping pattern during courtship: the two fish concurrently produce series of small chirps before the female generates a long chirp. The long chirp is acknowledged by the male with a chirp-doublet that in turn is often followed by one or more small chirps emitted by the female. For statistics see text, Fig. 5, Fig. 5 – 2, and Fig. 6.

203 **Electrocommunication in the wild** We focused on two relevant communication situations, i.e., courtship and  
 204 aggressive dyadic interactions. In total, we detected 54 episodes of short-distance interactions that we interpreted as  
 205 courtship (see below) between low-frequency females (EOD $f$  < 750 Hz,  $n=2$ ) and high-frequency males (EOD $f$  >  
 206 750 Hz,  $n = 6$ ) (Meyer et al., 1987), occurring in 2 out of 5 nights. Courting was characterized by extensive  
 207 production of chirps (Fig. 2 A) by both males and females — with up to 8 400 chirps per individual per night  
 208 (Fig. 4). Most chirps were so-called “small chirps”, characterized by short duration (< 20 ms) EOD $f$  excursions  
 209 of less than 150 Hz and minimal reduction in EOD amplitude (Engler and Zupanc, 2001) (Fig. 1 B and Fig. 3).  
 210 Only females emitted an additional type of chirp in courtship episodes, the “long chirp” (Fig. 1 B and Fig. 3),  
 211 with a duration of  $162 \pm 39$  ms ( $n = 54$ ), a large EOD $f$  excursion of about 400 Hz, and a strong decrease in EOD  
 212 amplitude (Hagedorn and Heiligenberg, 1985). Per night and female we observed 9 and 45 long chirps, respectively,  
 213 generated every 3 to 9 minutes (1st and 3rd quartile), between 7 pm and 1 am (Fig. 4 A). Occasionally, courtship  
 214 was interrupted by intruding males, leading to aggressive interactions between resident and intruder males (see  
 215 below).

216 **Courtship chirping** Roaming males approached and extensively courted females by emitting large numbers of  
 217 small chirps (Fig. 4 A). Courtship communication was highly structured, with female long chirps playing a central  
 218 role. Long chirps were preceded by persistent emission of small chirps by the male with rates of up to 3 Hz  
 219 (Figs. 5 A, C and 5 – 2). Immediately before the long chirp, the female small-chirp rate tripled from below 1 Hz to  
 220 about 3 Hz within a few seconds. The male chirp rate followed this increase until the concurrent high-frequency  
 221 chirping of both fish ceased after the female long chirp. These chirp episodes were characterized by close proximity

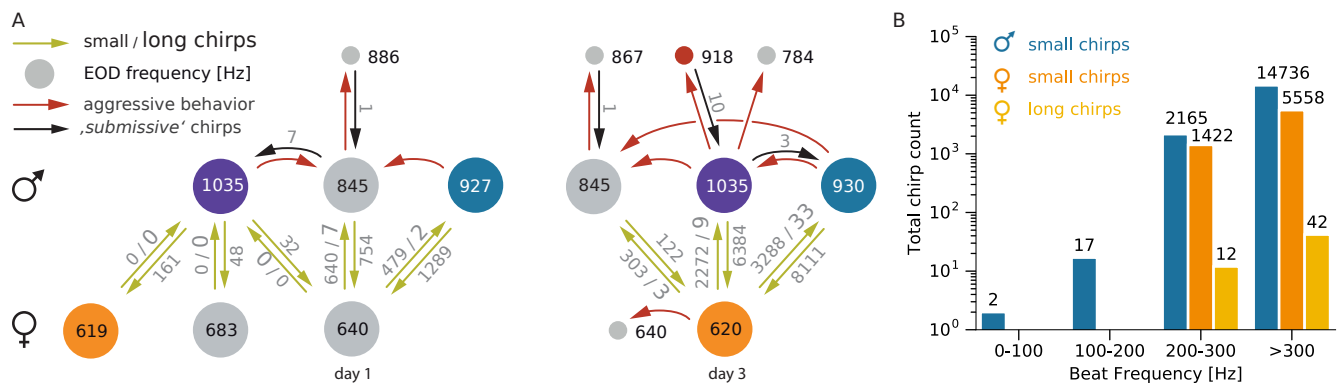


Figure 4: Social interactions and chirping. A) Ethogram of interactions of *A. rostratus* individuals (colored circles). The ethogram is based on data from 2012-05-10 (night 1) and 2012-05-12 (night 3) and illustrates the number and EOD frequencies of interacting fish as well as the number of emitted chirps that have been analyzed in this study. The numbers within circles indicate the EOD $f$ s of each fish in Hertz. Fish with similar EOD $f$ s on day 1 and day 3 may have been the same individuals. Green arrows and associated numbers indicate the numbers of small chirps and long chirps emitted in close proximity (<50 cm). Red arrows indicate aggressive behaviors, and black arrows the number of small chirps emitted during aggressive interactions. B) Histogram of chirp counts as a function of beat frequency (bin-width: 100 Hz). Note logarithmic scale used for chirp counts.

222 of the two fish (< 30 cm, Fig. 5 B, D). Long chirps were consistently acknowledged by males with a doublet of  
 223 small chirps (Fig. 3) emitted  $229 \pm 31$  ms after long chirp onset ( $n = 53$  measured in 5 pairs of interacting fish,  
 224 Fig. 4 A). The two chirps of the doublet were separated by only  $46 \pm 6$  ms, more than seven-fold shorter than the  
 225 most prevalent chirp intervals (Fig. 5 – 1). Finally, the female often responded with a few more loosely timed small  
 226 chirps about  $670 \pm 0.182$  ms after the long chirp (time of first chirp observed in  $n = 33$  of the 40 episodes shown in  
 227 Fig. 5 – 2). The concurrent increase in chirp rate, its termination by the female long chirp, the male doublet, and  
 228 the final response by small chirps of the female stood out as a highly stereotyped communication motif that clearly  
 229 indicates fast interactive communication.

230 **Males echo female chirps** On a sub-second timescale, male chirping was modulated by the timing of female  
 231 chirps (Figs. 6 A, C). Following a female small chirp, male chirp probability first decreased to a minimum at about  
 232 75 ms (significant in 4 out of 5 pairs of fish) and subsequently increased to a peak at about 165 ms (significant in 4  
 233 out of 5 pairs of fish). In contrast to males, females did not show any echo response (Figs. 6 B, D) — they timed  
 234 their chirps independently of the males' chirps.

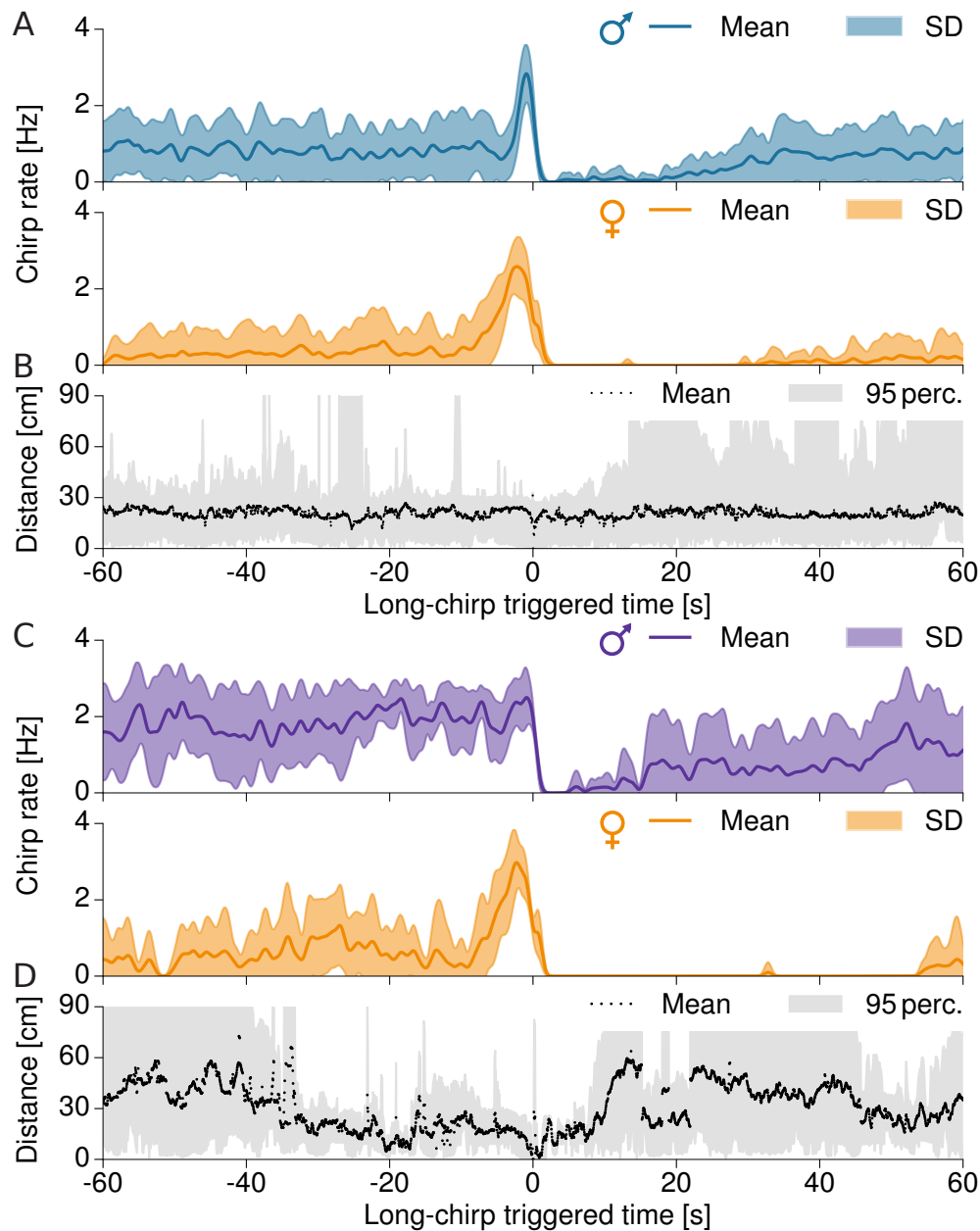


Figure 5: Temporal structure of courtship chirping of two example pairs. A) Average rate of small chirps of a male (top,  $EODf = 930$  Hz) courting a female (bottom,  $EODf = 620$  Hz,  $n = 32$  episodes, same pair as in Fig. 3, beat frequency is 310 Hz). B) Corresponding distance between the courting male and female. C, D) Same as in A and B for the pair shown in Fig. 2 (same female as in panel A and B, male  $EODf = 1035$  Hz, beat frequency 415 Hz,  $n = 8$  episodes). Time zero marks the female long chirp. Bands mark 95%-percentiles. See Fig. 5–2 for corresponding raster plots of small chirps.

Extended data:

Figure 5–1: Interchirp-interval distributions of small chirps.

Figure 5–2: Raster plots of small chirps.

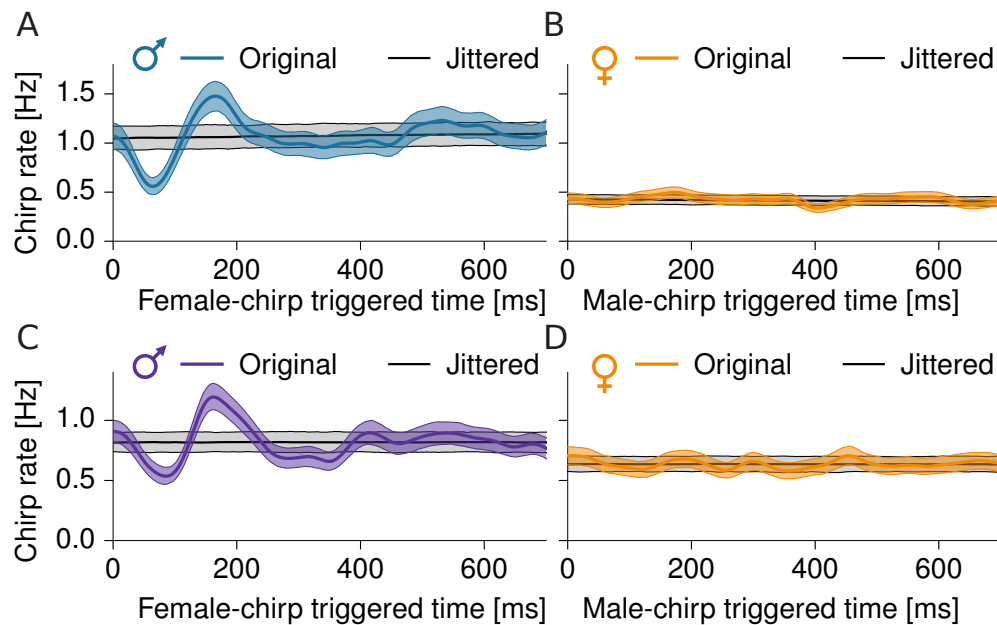


Figure 6: Fine structure of courtship chirping. Shown are cross-correlograms of chirp times, i.e. chirp rate of one fish relative to each chirp of the other fish (median with 95% confidence interval in color), of the same courting pairs of fish as in Fig. 5. Corresponding chirp rates and confidence intervals from randomly jittered, independent chirp times are shown in gray. A, C) Male chirping is first significantly inhibited immediately after a female chirp (A: at 64 ms, Cohen's  $d = 9.3$ ,  $n = 2565$  female chirps, C: at 85 ms, Cohen's  $d = 7.1$ ,  $n = 3213$  female chirps) and then transiently increased (A: at 166 ms,  $d = 5.9$ , C: at 162 ms,  $d = 7.5$ ). B, D) Female chirps are timed independently of male chirps (B: maximum  $d = 2.8$ ,  $n = 2648$  male chirps, D: maximum  $d = 1.9$ ,  $n = 2178$  male chirps).

235 **Competition between males** A second common type of electro communication interaction observed in our field  
 236 data was aggressive encounters between males competing for access to reproductively active females. These ag-  
 237 gressive interactions were triggered by intruding males that disrupted courtship of a resident, courting dyad. In-  
 238 truding males initially often lingered at distances larger than 70 cm from the courting dyad (8 of 16 scenes, median  
 239 duration 58.5 s; e.g., Fig. 2 A, movie M 2), consistent with assessment behavior (Arnott and Elwood, 2008). Resi-  
 240 dent males detected and often attacked intruders over distances of up to 177 cm, showing a clear onset of directed  
 241 movement toward the intruder (Fig. 2 C, movie M 2). In 5 out of 12 such situations a few small chirps indistin-  
 242 guishable from those produced during courtship were emitted exclusively by the retreating fish (Fig. 4 A). The  
 243 distances at which resident males started to attack intruders ranged from 20 cm to 177 cm ( $81 \pm 44$  cm,  $n = 10$ ,  
 244 Fig. 2 B, movie M 3). At the largest observed attack distance of 177 cm, the electric field strength was estimated  
 245 to be maximally  $0.34 \mu\text{V}/\text{cm}$  (assuming the fish were oriented optimally) — a value close to minimum behavioral  
 246 threshold values of about  $0.3 - 0.1 \mu\text{V}/\text{cm}$  measured in the laboratory at the fish's best frequency (Knudsen, 1974;

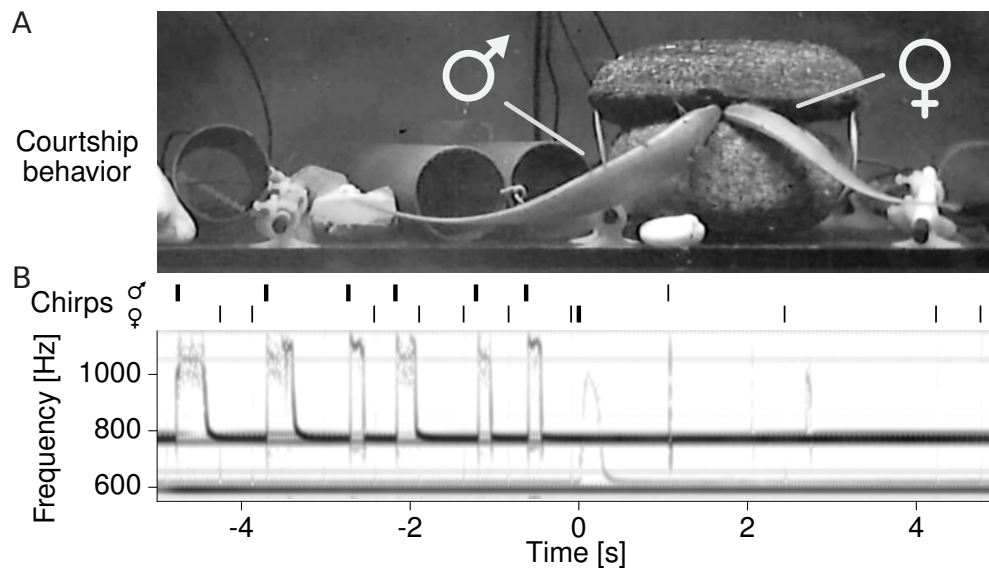


Figure 7: Synchronizing role of the female long chirp in spawning. A) Simultaneous video (snapshot of movie [M 4](#)) and B) voltage recordings (spectrogram) of *A. leptorhynchus* in the laboratory demonstrate the synchronizing function of the female long chirp (at time zero; trace with  $EODf = 608$  Hz baseline frequency) in spawning. In contrast to *A. rostratus*, male *A. leptorhynchus* generate an additional, long chirp type before spawning (top trace with  $EODf = 768$  Hz baseline frequency). Chirp onset times of the male and the female are marked by vertical bars above the spectrogram. Thick and thin lines indicate long and short duration chirps, respectively.

247 [Bullock et al., 1972](#)). We observed a single rise, a slow, gradual increase in  $EODf$  ([Zakon et al., 2002](#)), emitted by  
 248 a retreating intruder fish.

249 **Synchronization of spawning** We investigated the role of the female long chirp in a breeding experiment in the  
 250 laboratory ([Kirschbaum and Schugardt, 2002](#)) by continuously recording and videotaping a group of 3 males and  
 251 3 females of the closely related species *A. leptorhynchus* ([de Santana and Vari, 2013](#)) over more than 5 months.  
 252 Scanning more than 1.3 million emitted chirps, we found 76 female long chirps embedded in communication  
 253 episodes closely similar to those observed in *A. rostratus* in the wild (compare Fig. 7 B with Fig. 3). Eggs were  
 254 only found after nights with long chirps (six nights). The number of eggs found corresponded roughly to the number  
 255 of observed long chirps, supporting previous anecdotal findings that *Apteronotus* females spawn single eggs during  
 256 courtship episodes ([Hagedorn and Heiligenberg, 1985](#)). The associated video sequences triggered on female long  
 257 chirps show that, before spawning, females swim on their side close to the substrate, e.g., a rock or a filter, while  
 258 the male hovers in the vicinity of the female and emits chirps continuously (movie [M 4](#)). In the last seconds before  
 259 spawning, the female starts to emit a series of chirps, whereupon the male approaches the female. A fraction

260 of a second before the female emits its long chirp, the male pushes the female and retreats almost immediately  
261 afterwards (Fig. 7). It seems highly likely that this short episode depicts the synchronized release of egg and sperm.

262 **Statistics of natural stimuli** In a final step, we deduced the statistics of natural electrosensory stimuli resulting  
263 from the observed communication behaviors of *A. rostratus* to be able to relate it to the known physiological  
264 properties of electrosensory neurons in the discussion. Superposition of a fish's EOD with that of a nearby fish  
265 results in a periodic amplitude modulation, a so-called beat. Both frequency and amplitude of the beat provide  
266 a crucial signal background for the neural encoding of communication signals (Benda et al., 2005; Marsat et al.,  
267 2012; Walz et al., 2014). The beat frequency is given by the difference between the two EODs and the beat  
268 amplitude equals the EOD amplitude of the nearby fish at the position of the receiving fish (Fotowat et al., 2013).

269 The EOD amplitude and thus the beat amplitude decay with distance. We measured this decay directly from the  
270 data recorded with the electrode array (Fig. 8 A). The median EOD field amplitude at 3 cm distance was 2.4 mV/cm  
271 (total range: 1.4–5.1 mV/cm). The electric field decayed with distance according to a power law with exponent  
272  $1.28 \pm 0.12$  ( $n = 9$ ). This is less than the exponent of 2 expected for a dipole, because the water surface and  
273 the bottom of the stream distort the field (Fotowat et al., 2013). Small and long chirps emitted during courtship  
274 and small chirps emitted by retreating intruder males occurred at small distances of less than 32 cm (Fig. 8 B). In  
275 contrast, two behaviors involving intruding males occurred at large distances (Fig. 8 C): (i) Intruding males initially  
276 often lingered at distances larger than 70 cm from the courting dyad ( $n = 8$ , median duration 58.5 s; e.g., Fig. 2 A,  
277 movie M 2), consistent with assessment behavior (Arnott and Elwood, 2008). (ii) The distances at which resident  
278 males started to attack intruders ranged from 20 cm to 177 cm ( $81 \pm 44$  cm,  $n = 10$ , Fig. 2 B, movie M 3). At the  
279 largest observed attack distance of 177 cm, we estimated the electric field strength to be maximally  $0.34 \mu\text{V}/\text{cm}$ ,  
280 assuming the fish were oriented optimally.

281 All courtship chirping occurred at high beat frequencies (205–415 Hz for the five pairs where the female emitted  
282 long chirps, Fig. 8 F and Fig. 4 B). High beat frequencies were not a rare occurrence as the probability distribution  
283 of 406 beat frequencies measured from encounters in 5 nights show (Fig. 8 E). From these the 183 male-female  
284 encounters resulted in beat frequencies ranging from 99 to 415 Hz. Same-sex interactions, on the other hand,  
285 resulted in low beat frequencies up to 245 Hz (Fig. 8 E). Encounters between females were more frequent than  
286 between males (187 female versus 36 male encounters). Female EODs ranged from 585 to 748 Hz and resulted in  
287 observed beat frequencies from 1 to 142 Hz. Beat frequencies of 49 Hz were the most frequent among the females  
288 ( $n = 187$ ). Male EOD frequencies, on the other hand, span a much larger range from 776 to 1040 Hz, resulting in  
289 a broad and flat distribution of beat frequencies spanning 12 to 245 Hz (peak at 98 Hz,  $n = 36$ ). This includes the

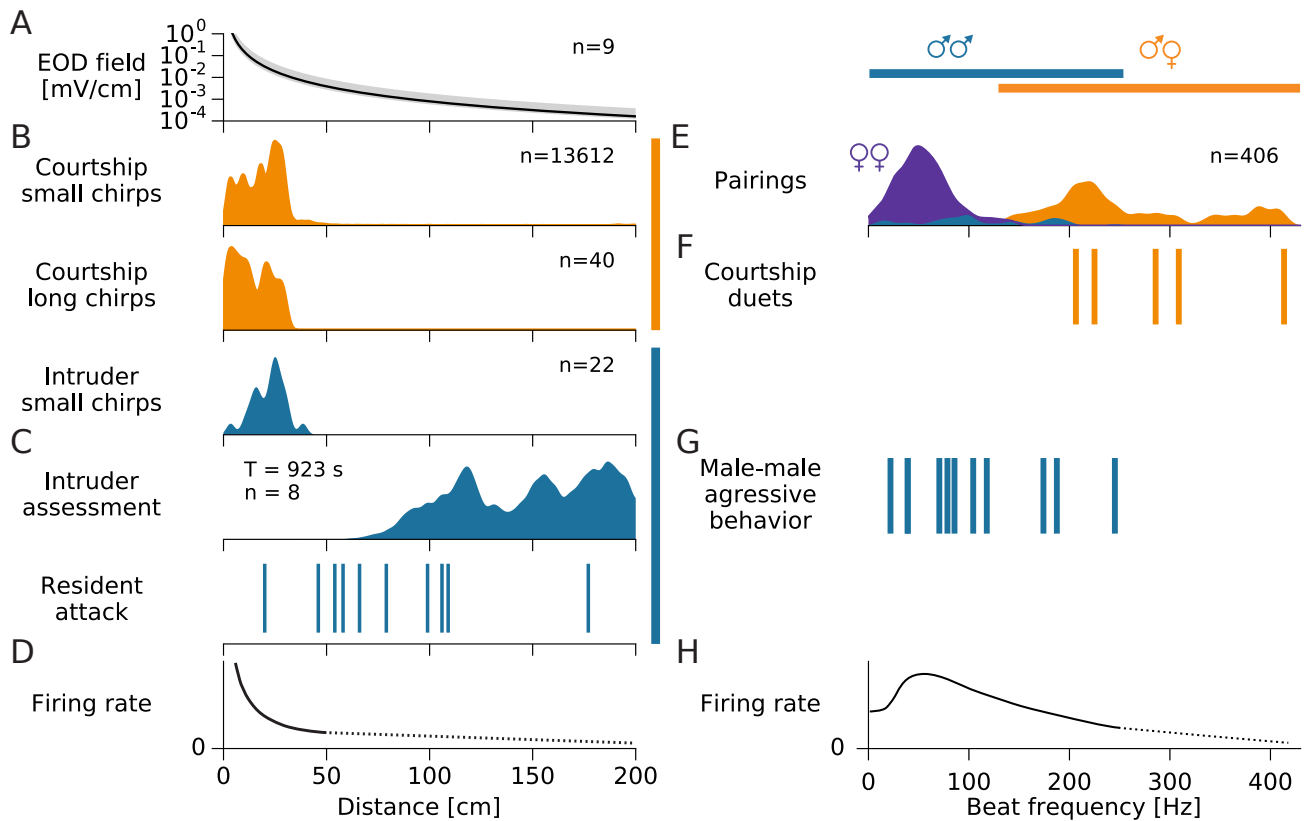


Figure 8: Statistics of behaviorally relevant natural stimuli. A) Maximum electric field strength as a function of distance from the emitting fish (median with total range). B) Small and long chirps in both courtship and aggression contexts are emitted consistently at distances below 32 cm. C) Intruder assessment and initiation of attacks by residents occur at much larger distances (movie M3). D) The firing rate response of P-unit afferents quickly decays with distance (solid line sketches data from Bastian, 1981a, Fig. 6). The dotted line is an extrapolation to so far not measured stimulus regimes. E) Distribution of beat frequencies of all *A. rostratus* appearing simultaneously in the electrode array. blue: male-male, violet: female-female, orange: male-female ( $n = 406$  pairings). F) Courtship behaviors occurred at beat frequencies in the range of 205–415 Hz. G) Aggressive interactions between males occurred at beat frequencies below 245 Hz. H) Sketch (solid line) and extrapolation (dotted line) of the tuning to beat frequencies of firing-rate responses of P-unit afferents based on Scheich et al. (1973); Bastian (1981a); Nelson et al. (1997); Benda et al. (2005); Walz et al. (2014).

290 range of beat frequencies observed at aggressive male-male interactions (Fig. 8 G).

## 291 **Discussion**

292 We recorded movement and electrocommunication signals in a wild population of the weakly electric fish, *Apteron-*  
293 *tus rostratus*, in their natural Neotropical habitat. A stereotyped pattern of interactive chirping climaxed in a special  
294 long chirp emitted by the female that we identified as a synchronizing signal for spawning. Courtship chirping was  
295 characterized by concurrent increases in chirp rate of both males and females on a tens-of-seconds time scale and  
296 by echo responses by the males on a 100 ms time scale. Courtship chirping occurred at distances below 32 cm  
297 and on high beat frequencies of up to 415 Hz. In contrast, aggressive interactions between males occurred at beat  
298 frequencies below about 200 Hz and often at distances larger than half a meter.

299 **Communication in the wild and in the laboratory** Our observations of male echo responses to female chirps  
300 (Figs. 6 A, C), precisely timed chirp doublets in response to female long chirps (Figs. 3), immediate behavioral  
301 reactions of males to female long chirps (Fig. 7, movie M4), and females slowly raising their chirp rate in response  
302 to male chirping and responding to the male's chirp doublet (Figs. 5 and 5 – 2) clearly qualify chirps as commu-  
303 nication signals in natural conditions. Laboratory studies have found echo responses on similar (Hupé and Lewis,  
304 2008) or slower time scales (Zupanc et al., 2006; Salgado and Zupanc, 2011; Metzen and Chacron, 2017) exclu-  
305 sively between males. Small chirps have been suggested to deter aggressive behavior (Hupé and Lewis, 2008).  
306 This is consistent with our observation of a submissive function of male-to-male chirping. The number of chirps  
307 generated in these aggressive contexts is, however, much lower (1 to 10 chirps in 5 of 9 pairings, Fig. 4) compared  
308 to encounters staged in laboratory tanks (about 125 chirps per 5 min trial (Hupé and Lewis, 2008)). Our field data  
309 do not support a function of chirps as signals of aggression and dominance (Triefenbach and Zakon, 2008). In  
310 particular the restricted space in laboratory experiments may explain these differences.

311 In so-called "chirp chamber" experiments, where a fish is restrained in a tube and is stimulated with artificial  
312 signals mimicking conspecifics, small chirps are predominantly generated by males at beat frequencies well below  
313 about 150 Hz, corresponding to same-sex interactions (Bastian et al., 2001; Engler and Zupanc, 2001). In contrast,  
314 in our observations of courting fish in the field and in the laboratory, both male and female fish almost exclusively  
315 chirped in male-female contexts at beat frequencies above about 200 Hz (Fig. 4 B).

316 **Electric synchronization of spawning by courtship-specific chirps** Our results provide strong evidence that  
317 female long chirps are an exclusive communication signal for the synchronization of egg and sperm release for

318 external fertilization as has been suggested by [Hagedorn and Heiligenberg \(1985\)](#): (i) The female long chirp was  
319 the central part of a highly stereotyped communication pattern between a courting duet (Figs. 3, 5, and 5). (ii)  
320 Fertilized eggs were found at the locations of male-female interaction, and only when the female had produced  
321 long chirps in the preceding night. (iii) The period immediately before the female long chirp was characterized  
322 by extensive chirp production by the male (Fig. 5). (iv) Video sequences triggered on female long chirps clearly  
323 demonstrated the special role of the female long chirp (Fig. 7, movie M4).

324 **Robust responses to communication signals** Male echo responses to female chirps occurring reliably within  
325 a few tens of milliseconds (Figs. 6 A, C), precisely timed chirp doublets (Figs. 3), and long-range assessment  
326 and attacks (Fig. 8 C) demonstrate that the respective electrocommunication signals are successfully and robustly  
327 evaluated by the electrosensory system, as it is expected for communication signals ([Wilson, 1975](#); [Endler, 1993](#)).  
328 The electrosensory signals arising in these interactions are dominated by beats, i.e. amplitude modulations arising  
329 from the interference of the individual electric fields.

330 Two types of tuberous electroreceptor afferents could contribute to the observed behavioral responses in *A.*  
331 *rostratus*. T-units play an important role in the jamming avoidance response ([Bullock et al., 1972](#); [Rose and](#)  
332 [Heiligenberg, 1985](#)). Whether and how T-units are able to encode beats with frequencies higher than 20 Hz is  
333 not known yet. P-units, the dominant type of tuberous receptors ([Carr et al., 1982](#)), encode amplitude modulations  
334 of the fish's EOD in their firing rate ([Scheich et al., 1973](#); [Bastian, 1981a](#); [Nelson et al., 1997](#); [Benda et al., 2005](#);  
335 [Walz et al., 2014](#)). Tuning of P-unit firing rate responses, spike-time correlations, and stimulus-response coherences  
336 to beat frequencies have been characterized up to beat frequencies of 300 Hz by single-unit, dual-unit, and nerve  
337 recordings ([Bastian, 1981a](#); [Nelson et al., 1997](#); [Benda et al., 2006](#); [Walz et al., 2014](#)). These measures are on  
338 average strongest at beat frequencies of about 30 to 130 Hz ([Bastian, 1981a](#); [Benda et al., 2006](#); [Walz et al., 2014](#);  
339 [Grewe et al., 2017](#)), covering well the beat frequencies arising from same-sex interactions (Fig. 8 G). For higher  
340 beat frequencies firing rate responses and related measures decay to very low values (Fig. 8 H).

341 **Neglected stimulus frequencies** Only very few studies have looked at P-unit responses to beat frequencies  
342 beyond 300 Hz, and none addressed the encoding of chirps beyond 250 Hz. Narrow-band amplitude modulations  
343 of up to 400 Hz were shown to evoke sizable stimulus-response coherences ([Savard et al., 2011](#)), and a recent study  
344 reported significant spike-time locking of P-units to beat frequencies up to 500 Hz ([Sinz et al., 2017](#)). Encoding  
345 of the low beat frequencies occurring during male-male interactions is thus well understood. However, we know  
346 very little about the processing of high beat frequencies as they occur during male-female interactions and we can  
347 only speculate about the encoding of chirps occurring on beat frequencies beyond 250 Hz as they occur in courtship

348 scenes.

349 The difference between the high beat frequencies that we observed during courtship interactions (205–415 Hz,  
350 Fig. 8 F and Fig. 4 B) and the peak of the frequency tuning of the firing rate (Fig. 8 H) is unexpected given the many  
351 examples of frequency-matched courtship signals in other sensory systems (e.g., Rieke et al., 1995; Machens et al.,  
352 2005; Kostarakos et al., 2009; Schrode and Bee, 2015). The high beat frequencies result from males having higher  
353 frequencies than females (Meyer et al., 1987). In the genus *Apteronotus* the presence, magnitude, and direction of  
354 EOD  $f$  dimorphism varies considerably across species and thus is evolutionarily labile (Smith, 2013).

355 **Encoding of low amplitude beats** The field strength of the EOD, and with it beat amplitude, decays with distance  
356 (Fig. 8 A). Most of the studies on P-unit coding, including Savard et al. (2011) and Sinz et al. (2017), used rather  
357 strong beat amplitudes of more than 10 % of the EOD amplitude. We observed chirp interactions at distances up  
358 to 32 cm, corresponding to beat amplitudes of about 1 % (Fig. 8 A). Opponent assessment and decision to attack  
359 usually occur at even larger distances (Fig. 8 C), where the relevant signal amplitudes are much smaller than 1% of  
360 the fish's own EOD amplitude. In general, smaller beat amplitudes result in down-scaled frequency tuning curves  
361 (Bastian, 1981a; Benda et al., 2006; Savard et al., 2011; Grewe et al., 2017), and reduced phase locking (Sinz et al.,  
362 2017). However, encoding of beats and chirps has so far only been studied for amplitudes larger than 1% (Bastian,  
363 1981a; Nelson et al., 1997).

364 **Decoding** P-units converge onto pyramidal cells in the electrosensory lateral line lobe (ELL) (Heiligenberg and  
365 Dye, 1982; Maler, 2009). The rate tuning curves of pyramidal cells peak at frequencies similar to or lower than  
366 those of P-units (Bastian, 1981b), and their stimulus-response coherences peak well below 100 Hz, but have only  
367 been measured up to 120 Hz (Chacron et al., 2003; Chacron, 2006; Krahe et al., 2008). Coding of small chirps  
368 by pyramidal cells in the ELL and at the next stage of processing, the Torus semicircularis, has so far only been  
369 studied at beat frequencies below 60 Hz (Marsat et al., 2009; Marsat and Maler, 2010; Vonderschen and Chacron,  
370 2011; Marsat et al., 2012; Metzen et al., 2016). Thus, most electrophysiological recordings from the electrosen-  
371 sory system have been biased to low beat frequencies and strong stimulus amplitudes evoking obvious neuronal  
372 responses, but overlooking the stimuli relevant for reproduction.

373 **Conclusion** Our observations regarding sex-specificity, numbers, and functions of chirps differ substantially from  
374 laboratory studies. The fish robustly responded to courtship signals that occurred on beat-frequencies that were un-  
375 expectedly high given previous, mainly laboratory-based findings on chirping (Smith, 2013; Walz et al., 2013).  
376 This range of stimulus frequencies has also been largely ignored by electrophysiological characterizations of the

377 electrosensory system. Our field data thus identify important — but so far neglected — stimulus regimes of the  
378 electrosensory system and provide further evidence for the existence of sensitive neural mechanisms for the detec-  
379 tion of such difficult sensory signals (Gao and Ganguli, 2015). Our work also points to the limitations of laboratory  
380 studies and emphasize the importance of research in the natural habitat, which opens new windows for understand-  
381 ing the real challenges faced and solved by sensory systems.

## 382 **References**

- 383 Arnott G, Elwood RW (2008) Information gathering and decision making about resource value in animal contests.  
384 *Anim Behav* 76:529–542.
- 385 Bastian J (1981a) Electrolocation I. How electroreceptors of *Apteronotus albifrons* code for moving objects and  
386 other electrical stimuli. *J Comp Physiol* 144:465–479.
- 387 Bastian J (1981b) Electrolocation II. The effects of moving objects and other electrical stimuli on the activities of  
388 two categories of posterior lateral line lobe cells in *Apteronotus albifrons*. *J Comp Physiol* 144:481–494.
- 389 Bastian J, Schniederjan S, Nguyenkim J (2001) Arginine vasotocin modulates a sexually dimorphic communication  
390 behavior in the weakly electric fish *Apteronotus leptorhynchus*. *J Exp Biol* 204:1909–1923.
- 391 Benda J, Longtin A, Maler L (2005) Spike-frequency adaptation separates transient communication signals from  
392 background oscillations. *J Neurosci* 25:2312–2321.
- 393 Benda J, Longtin A, Maler L (2006) A synchronization-desynchronization code for natural communication signals.  
394 *Neuron* 52:347–358.
- 395 Bullock TH, Hamstra RH, Scheich H (1972) The jamming avoidance response of high frequency electric fish. II.  
396 Quantitative aspects. *J Comp Physiol* 77:23–48.
- 397 Carr CE, Maler L, Sas E (1982) Peripheral organization and central projections of the electrosensory nerves in  
398 gymnotiform fish. *J Comp Neurol* 211:139–153.
- 399 Chacron MJ (2006) Nonlinear information processing in a model sensory system. *J Neurophysiol* 95:2933–2946.
- 400 Chacron MJ, Doiron B, Maler L, Longtin A, Bastian J (2003) Non-classical receptive field mediates switch in a  
401 sensory neuron’s frequency tuning. *Nature* 423:77–81.
- 402 Clemens J, Ronacher B (2013) Feature extraction and integration underlying perceptual decision making during  
403 courtship behavior. *J Neurosci* 33:12136–12145.
- 404 Egnor SER, Branson K (2016) Computational Analysis of Behavior. *Annu Rev Neurosci* 39:217–236.
- 405 Endler JA (1993) Some General Comments on the Evolution and Design of Animal Communication Systems. *Phil*

- 406 Trans R Soc Lond B 340:215–225.
- 407 Engler G, Zupanc GK (2001) Differential production of chirping behavior evoked by electrical stimulation of the  
408 weakly electric fish, *Apteronotus leptorhynchus*. J Comp Physiol A 187:747–756.
- 409 Fotowat H, Harrison RR, Krahe R (2013) Statistics of the electrosensory input in the freely swimming weakly  
410 electric fish *Apteronotus leptorhynchus*. J Neurosci 33:13758–13772.
- 411 Froudarakis E, Berens P, Ecker AS, Cotton RJ, Sinz FH, Yatsenko D, Saggau P, Bethge M, Tolias AS (2014) Pop-  
412 ulation code in mouse V1 facilitates readout of natural scenes through increased sparseness. Nature Neurosci  
413 17:851–857.
- 414 Fugère V, Ortega H, Krahe R (2011) Electrical signalling of dominance in a wild population of electric fish. Biol  
415 Lett 7:197–200.
- 416 Gao P, Ganguli S (2015) On simplicity and complexity in the brave new world of large-scale neuroscience. Curr  
417 Opin Neurobiol 33:666–670.
- 418 Gollisch T, Meister M (2010) Eye smarter than scientists believed: neural computations in circuits of the retina.  
419 Neuron 65:150–164.
- 420 Grewe J, Kruscha A, Lindner B, Benda J (2017) Synchronous spikes are necessary but not sufficient for a synchrony  
421 code in populations of spiking neurons. PNAS 114:E1977–E1985.
- 422 Hagedorn M, Heiligenberg W (1985) Court and spark: electric signals in the courtship and mating of gymnotid  
423 fish. Anim Behav 33:254–265.
- 424 Heiligenberg W, Dye J (1982) Labelling of electroreceptive afferents in a gymnotoid fish by intraeellular injection  
425 of HRP: the mystery of multiple maps. J Comp Physiol 148:287–296.
- 426 Henninger J (2015) Social interactions in natural populations of weakly electric fish. dissertation, Eberhard Karls  
427 Universität Tübingen.
- 428 Hopkins CD (1973) Lightning as background noise for communication among electric fish. Nature 242:268–270.
- 429 Hupé GJ, Lewis JE (2008) Electrocommunication signals in free swimming brown ghost knifefish, *Apteronotus*  
430 *leptorhynchus*. J Exp Biol 211:1657–1667.
- 431 Kirschbaum F, Schugardt C (2002) Reproductive strategies and developmental aspects in mormyrid and gymnoti-  
432 form fishes. J Physiol Paris 96:557–566.
- 433 Knudsen EI (1974) Behavioral thresholds to electric signals in high frequency electric fish. J Comp Physiol A  
434 91:333–353.
- 435 Kostarakos K, Hennig MR, Römer H (2009) Two matched filters and the evolution of mating signals in four species  
436 of cricket. Front Zool 6:22.

- 437 Krahe R, Bastian J, Chacron MJ (2008) Temporal processing across multiple topographic maps in the electrosen-  
438 sory system. *J Neurophysiol* 100:852–867.
- 439 Laughlin S (1981) A simple coding procedure enhances a neuron's information capacity. *Z Naturforsch C* 36:910–  
440 912.
- 441 Lewicki MS, Olshausen BA, Surlykke A, Moss CF (2014) Scene analysis in the natural environment. *Front Psychol*  
442 5:1–21.
- 443 Machens CK, Gollisch T, Kolesnikova O, Herz AVM (2005) Testing the efficiency of sensory coding with optimal  
444 stimulus ensembles. *Neuron* 47:447–456.
- 445 Maler L (2009) Receptive field organization across multiple electrosensory maps. I. Columnar organization and  
446 estimation of receptive field size. *J Comp Neurol* 516:376–393.
- 447 Marsat G, Longtin A, Maler L (2012) Cellular and circuit properties supporting different sensory coding strategies  
448 in electric fish and other systems. *Curr Opin Neurobiol* 22:1–7.
- 449 Marsat G, Maler L (2010) Neural heterogeneity and efficient population codes for communication signals. *J Neu-*  
450 *rophysiol* 104:2543–2555.
- 451 Marsat G, Proville RD, Maler L (2009) Transient signals trigger synchronous bursts in an identified population of  
452 neurons. *J Neurophysiol* 102:714–723.
- 453 Metzen MG, Chacron MJ (2017) Stimulus background influences phase invariant coding by correlated neural  
454 activity. *eLife* 6:e24482.
- 455 Metzen MG, Hofmann V, Chacron MJ (2016) Neural correlations enable invariant coding and perception of natural  
456 stimuli in weakly electric fish. *eLife* 5:e12993.
- 457 Meyer JH, Leong M, Keller CH (1987) Hormone-induced and maturational changes in electric organ discharges  
458 and electroreceptor tuning in the weakly electric fish *Apteronotus*. *J Comp Physiol A* 160:385–394.
- 459 Nelson ME, MacIver MA (1999) Prey capture in the weakly electric fish *Apteronotus albifrons*: sensory acquisition  
460 strategies and electrosensory consequences. *J Exp Biol* 202:1195–1203.
- 461 Nelson ME, Xu Z, Payne JR (1997) Characterization and modeling of P-type electrosensory afferent responses to  
462 amplitude modulations in a wave-type electric fish. *J Comp Physiol A* 181:532–544.
- 463 Olshausen BA, Field DJ (1996) Emergence of simple-cell receptive-field properties by learning a sparse code for  
464 natural images. *Nature* 381:607–609.
- 465 Olshausen BA, Field DJ (2005) How close are we to understanding V1? *Neural Comput* 17:1665–1699.
- 466 Rieke F, Bodnar DA, Bialek W (1995) Naturalistic stimuli increase the rate and efficiency of information transmis-  
467 sion by primary auditory afferents. *Proc R Soc Lond B* 262:259–265.

- 468 Rose G, Heiligenberg W (1985) Temporal hyperacuity in the electric sense of fish. *Nature* 318:178–180.
- 469 Salgado JAG, Zupanc GKH (2011) Echo response to chirping in the weakly electric brown ghost knifefish  
470 (*Apteronotus leptorhynchus*): role of frequency and amplitude modulations. *Can J Zool* 89:498–508.
- 471 de Santana CD, Vari RP (2013) Brown ghost electric fishes of the *Apteronotus leptorhynchus* species-group (Os-  
472 tarioptysi, Gymnotiformes); monophyly, major clades, and revision. *Zool J Linnean Soc* 168:564–596.
- 473 Savard M, Krahe R, Chacron MJ (2011) Neural heterogeneities influence envelope and temporal coding at the  
474 sensory periphery. *Neurosci* 172:270–284.
- 475 Scheich H, Bullock TH, Robert H Hamstra J (1973) Coding properties of two classes of afferent nerve fibers: high  
476 frequency electroreceptors in the electric fish, *Eigenmannia*. *J Neurophysiol* 36:39–60.
- 477 Schrode KM, Bee MA (2015) Evolutionary adaptations for the temporal processing of natural sounds by the anuran  
478 peripheral auditory system. *J Exp Biol* 218:837–848.
- 479 Sinz FH, Sachgau C, Henninger J, Benda J, Grewe J (2017) Simultaneous spike-time locking to multiple frequen-  
480 cies. *bioRxiv*.
- 481 Smith EC, Lewicki MS (2006) Efficient auditory coding. *Nature* 439:978–982.
- 482 Smith GT (2013) Evolution and hormonal regulation of sex differences in the electrocommunication behavior of  
483 ghost knifefishes (Apteronotidae). *J Exp Biol* 216:2421–33.
- 484 Stamper SA, Carrera-G E, Tan EW, Fugère V, Krahe R, Fortune ES (2010) Species differences in group size and  
485 electrosensory interference in weakly electric fishes: implications for electrosensory processing. *Behav Brain*  
486 *Res* 207:368–376.
- 487 Theunissen FE, Sen K, Doupe AJ (2000) Spectral-temporal receptive fields of nonlinear auditory neurons obtained  
488 using natural sounds. *The Journal of Neuroscience* 20:2315–2331.
- 489 Triefenbach FA, Zakon H (2008) Changes in signalling during agonistic interactions between male weakly electric  
490 knifefish, *Apteronotus leptorhynchus*. *Anim Behav* 75:1263–1272.
- 491 Vonderschen K, Chacron MJ (2011) Sparse and dense coding of natural stimuli by distinct midbrain neuron sub-  
492 populations in weakly electric fish. *J Neurophysiol* 106:3102–3118.
- 493 Walz H, Grewe J, Benda J (2014) Static frequency tuning properties account for changes in neural synchrony  
494 evoked by transient communication signals. *J Neurophysiol* 112:752–765.
- 495 Walz H, Hupé G, Benda J, Lewis JE (2013) The neuroethology of electrocommunication: how signal background  
496 influences sensory encoding and behaviour in *Apteronotus leptorhynchus*. *J Physiol Paris* 107:13–25.
- 497 Wilson EO (1975) *Sociobiology: the new synthesis*. Cambridge MA: Harvard University Press.
- 498 Zakon HH, Oestreich J, Tallarovic S, Triefenbach F (2002) EOD modulations of brown ghost electric fish: JARs,

499 chirps, rises, and dips. *J Physiol Paris* 96:451–458.

500 Zupanc GKH, Sîrbulescu RF, Nichols A, Ilies I (2006) Electric interactions through chirping behavior in the weakly  
501 electric fish, *Apteronotus leptorhynchus*. *J Comp Physiol A* 192:159–173.

## 502 **Multimedia files**

### 503 **Audio**

**Audio A 1:** Audio trace of the courtship sequence shown in Fig. 3. A male ( $EOD_f = 930$  Hz) generated a series of small chirps. Eventually, the female ( $EOD_f = 620$  Hz) fish joins in, increases chirp rate and finishes with a long chirp, which is acknowledged by the male with a small chirp doublet.

File: audio\_courtship.wav

### 504 **Animations and Video**

**Movie M 1:** Example of raw voltage recordings and corresponding position estimates of a single fish, *Eigenmannia humboldtii*, passing through the array of electrodes. The head and tail area of its electric field are of opposite polarity, which is why the polarity of the recorded EOD switches as the fish passes an electrode. Note the large electric spikes occurring irregularly on all electrodes. Previous studies (Hopkins, 1973) attributed similar patterns to propagating distant lightning. The animation is played back at real-time.

File: movie\_raw\_and\_position.avi

**Movie M2:** Animation of the courtship and aggression behavior shown in Fig. 2. A courting dyad is engaged in intense chirp activity (transparent circles and 50 ms beeps at the fish's baseline  $EOD_f$ ). An intruder male (red circles indicate positions of the last 5 seconds, black circles mark current positions) first lingers at a distance of one meter. When it approaches further, courting is interrupted and the resident male engages the intruder. Just before the male intruder retreats, it emits a series of small chirps, and subsequently leaves the recording area. The resident male returns to the female and resumes chirping. Eventually, the female responds with small chirps followed by a single long chirp (large open circle and a 500 ms beep at the female's baseline  $EOD_f$ ). Then both fish cease chirp activity and the male resumes to emit chirps after a few seconds. The animation is played back at  $2\times$  real-time.

File: movie\_intruder.avi

**Movie M3:** Animation of a courtship sequence with multiple attempts of an intruding male to approach the courting dyad. The resident male drives the intruder away three times, starting the approach at increasingly greater distances. *Apteronotus rostratus* are marked by circles, *Eigenmannia humboldtii* by squares. The animation is played back at 2× real-time.

File: movie\_repetitive\_intruder.avi

**Movie M4:** Spawning of the closely related species *Apteronotus leptorhynchus* during a breeding experiment. The overall sequence of chirp production is very similar to the courtship motif observed in *A. rostratus*. However, male *A. leptorhynchus* increasingly generate a second type of chirp, a variety of a long chirp, as spawning approaches. The video shows a big male (EOD  $f = 770$  Hz) courting a smaller female (590 Hz). The audio signal was created from concurrent EOD recordings. Both fish generate chirps at an increased rate (about 1.5 Hz), just before the male thrusts its snout against the female, which responds with a long chirp, clearly noticeable from the audio trace. Subsequently, the male retreats to a tube and the female hovers around the substrate, where the spawned egg was found.

File: movie\_spawning.avi

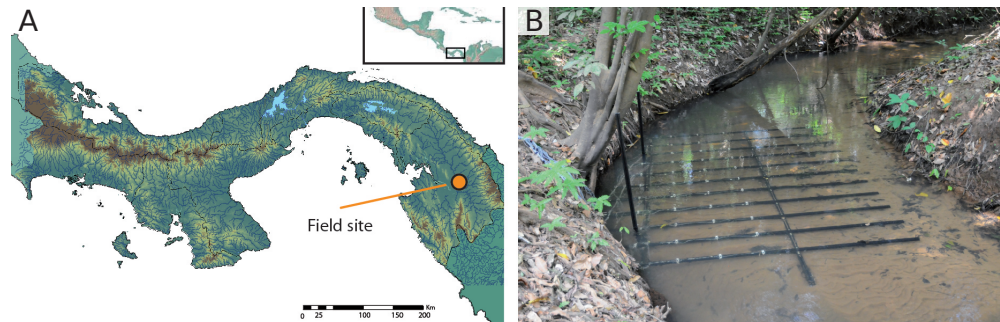
505 **Extended data**

Figure 1 – 1: Field site and the electrode array positioned in a stream. A) The field data were recorded in the Darién province in Eastern Panamá. B) The electrode array covered  $2.4 \times 1.5 \text{ m}^2$  of our recording site in a small quebrada of the Chucunaque River system. Electrodes (on white electrode holders) were positioned partly beneath the excavated banks, allowing to record electric fish hiding deep in the root masses.

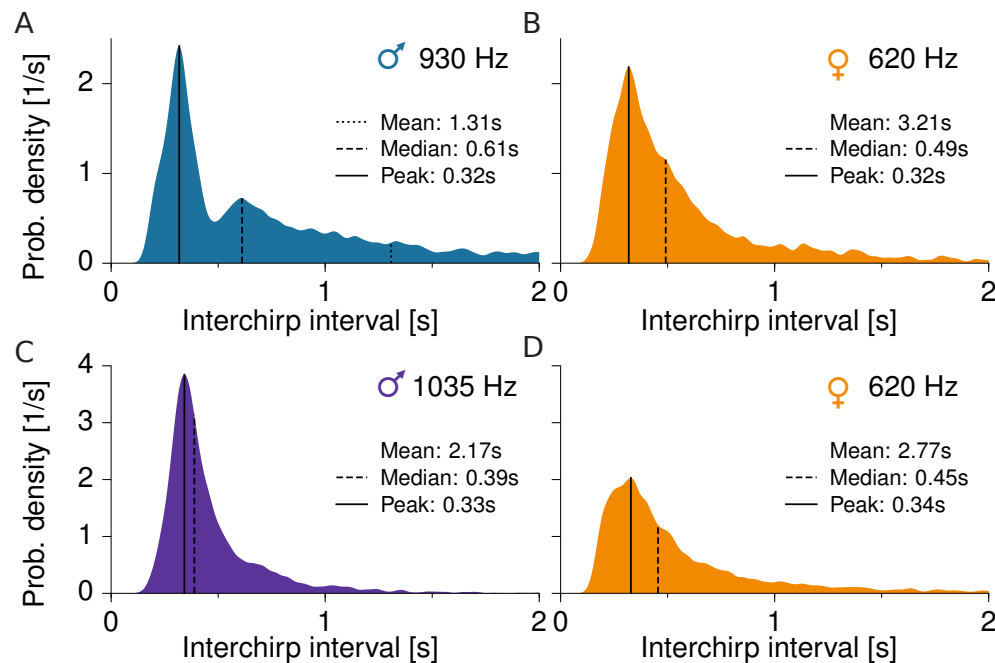


Figure 5 – 1: Interchirp-interval distributions of small chirps underlying the chirbrates shown in fig. 5. A) Male with  $\text{EOD}f = 930 \text{ Hz}$  ( $n = 8439$  small chirps). B) Female with  $\text{EOD}f = 620 \text{ Hz}$  ( $n = 3431$ ). C) Another male with  $\text{EOD}f = 1035 \text{ Hz}$  ( $n = 6857$ ). D) Same female as in panel B ( $n = 5336$  chirps).

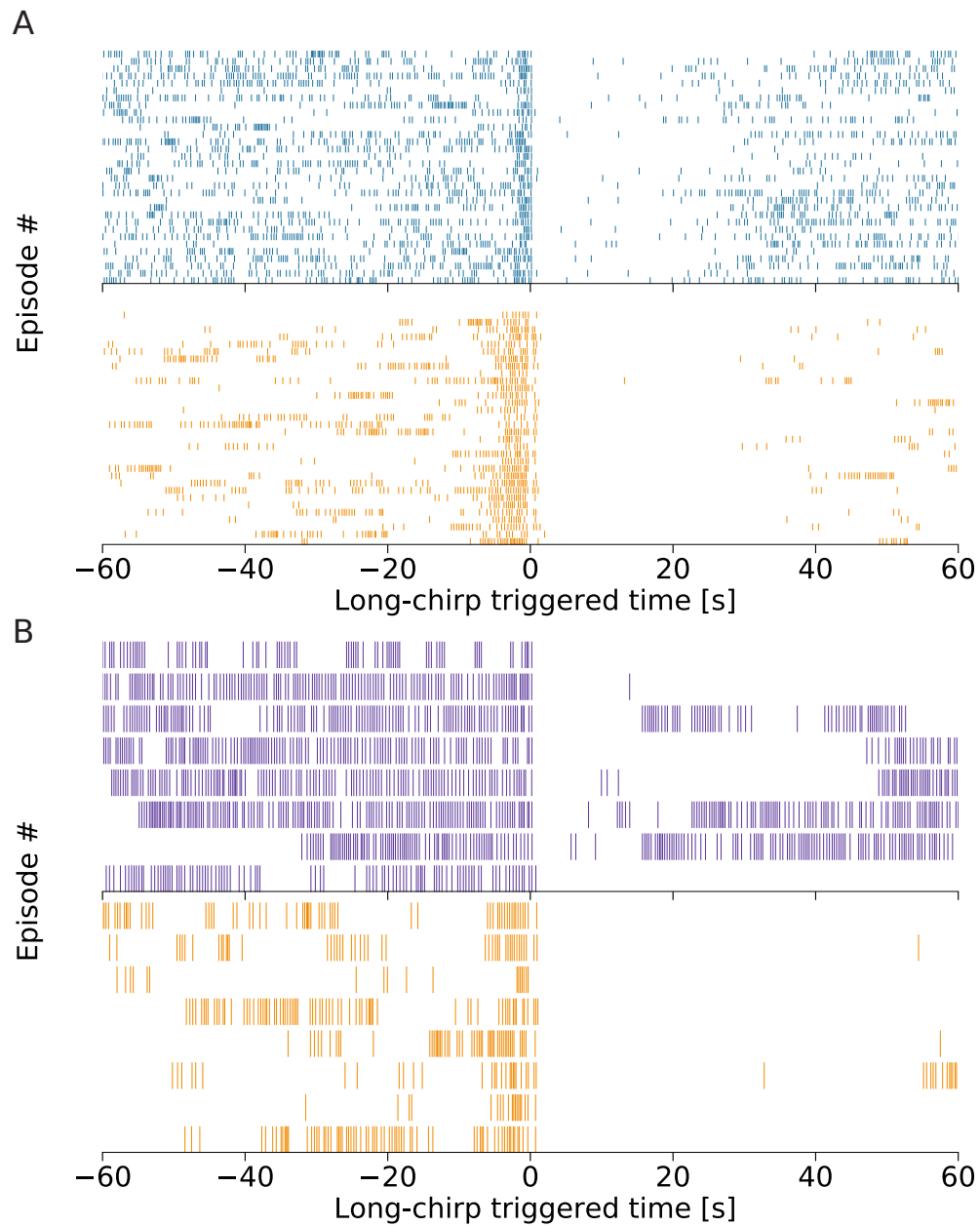


Figure 5 – 2: Raster plots of small chirps underlying the chirprates shown in fig. 5. A) Male with  $EODf = 930$  Hz (top) and female with  $EODf = 620$  Hz (bottom). B) Another male with  $EODf = 1035$  Hz (top) and same female as in panel A (bottom). Each row corresponds to a single courtship episode, each stroke marks a small chirp.